^{18}F-FDG autoradiography enhancement with CMOS sensor

Truong Nguyen Pham, Virgile Bekaert, Christian Finck, Patrice Marchand, David Brasse, Frédéric Boisson, Patrice Laquerriere

Département Radiobiologie, Hadronthérapie et Imagerie Moléculaire

Université de Strasbourg, CNRS, IPHC UMR 7178, F-67000 Strasbourg, France

truong.nguyen-pham@iphc.cnrs.fr

ICISE QUY NHON VIETNAM

Outline

- Introduction
- Materials and methods
- Results and discussion
- Conclusions and perspective

Introduction

Context

- Positron emission tomography (PET):
  - functional imaging
  - pico-molar detection
  - spatial resolution 1 mm in preclinical research

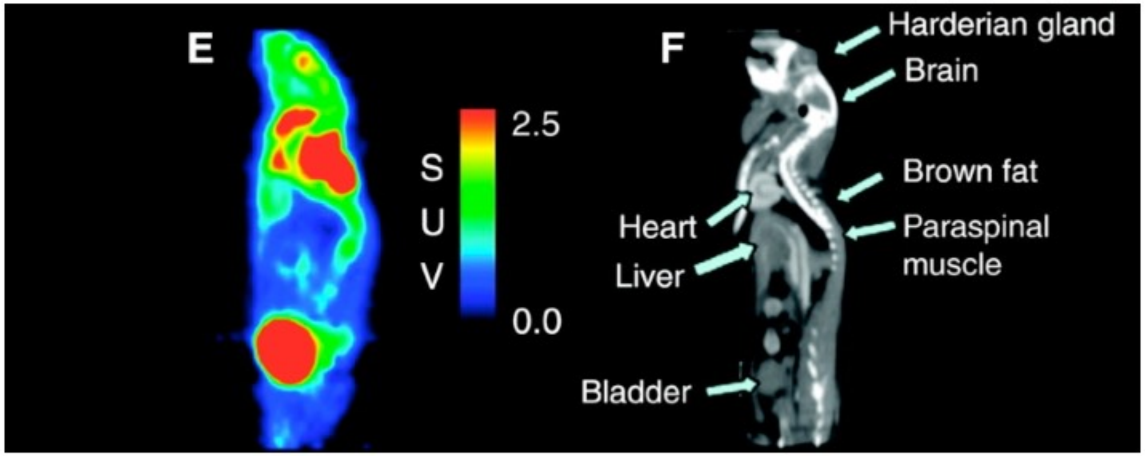

Biodistribution of 18F-FDG for a mouse: not fasted, not warmed, no anesthesia.

Fueger, Barbara J., et al. *Journal of Nuclear Medicine*. 2006

Introduction

Context

- Biodistribution at brain scale?
- Limitation of the spatial resolution
- System with sub-millimeter resolution scale and good sensitivity

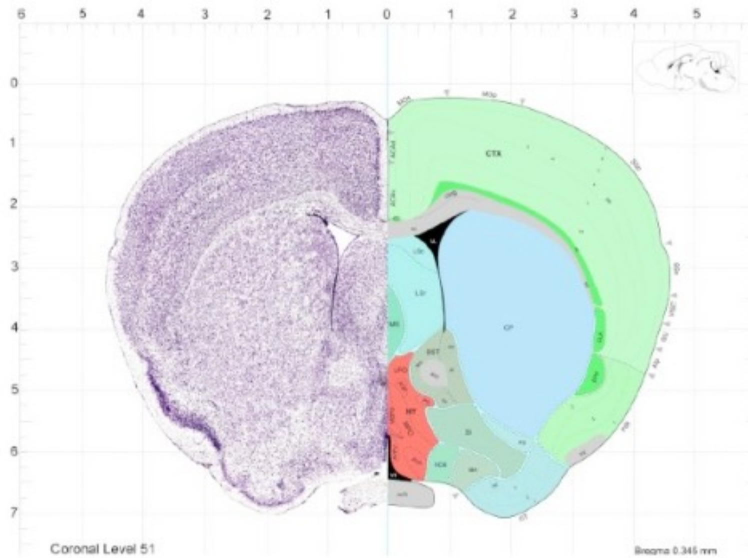

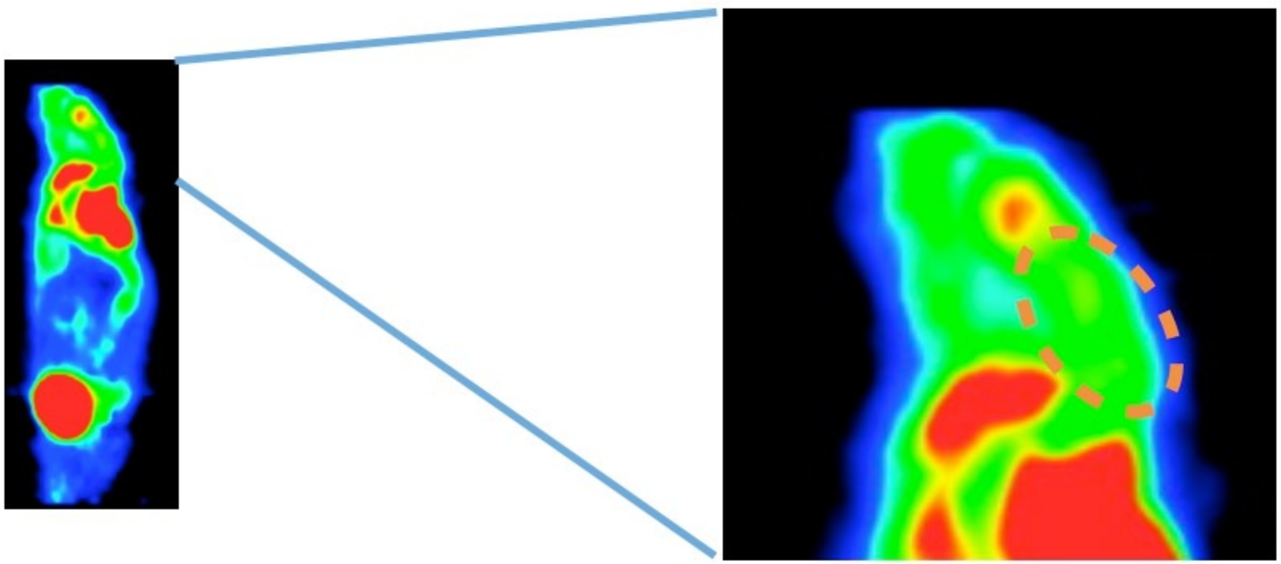

Homogenous or specific uptake?

Fueger, Barbara J., et al. *Journal of Nuclear Medicine*. 2006

Introduction

Context

- Autoradiography, a method to map the 2D distribution in a radiolabeled <u>*ex-vivo*</u> tissue

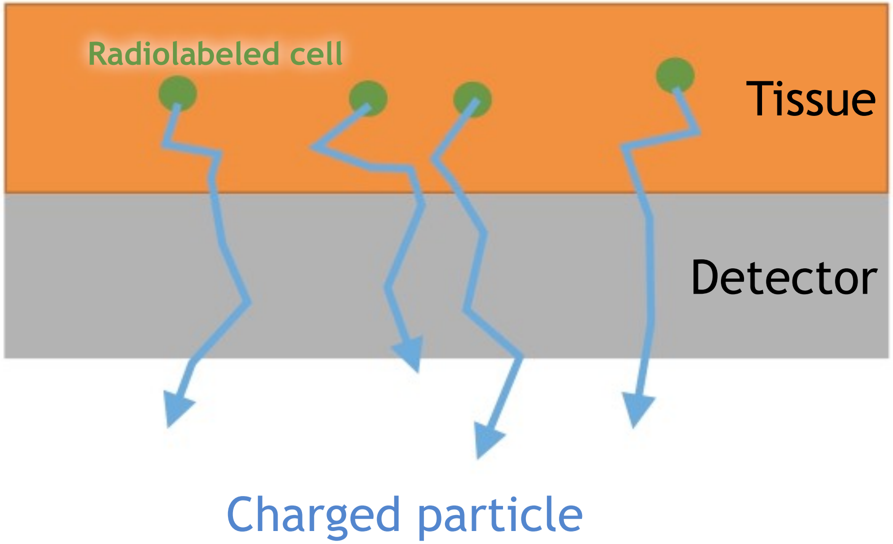

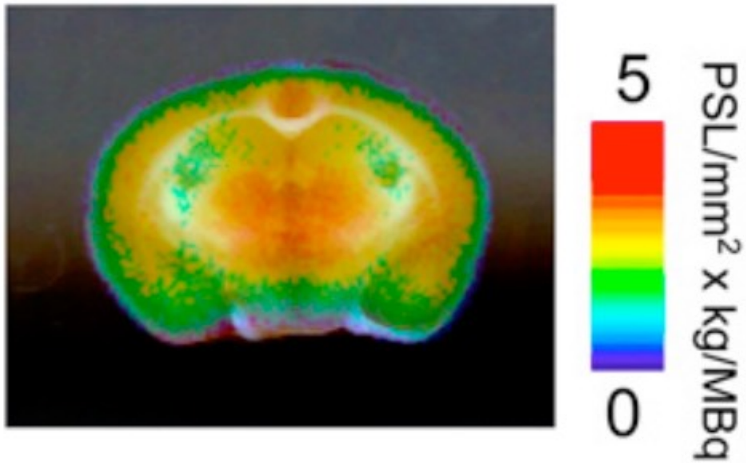

Distribution of ^{18}F-FDG in a mouse with phosphor plate.

Mizuma, Hiroshi, et al. *Journal of Nuclear Medicine*. 2010

Introduction

State of art autoradiography

Technique AR	Activity injected per acquisition time	Spatial resolution	Author
Emulsion film	0.77 MBq/min	4 µm	Yamada, S. et al, Neuroscience letters, 1990.
Phosphor imaging plate	1 MBq/min	330 µm	Mizuma, H. et al, Journal of Nuclear Medicine, 2010.
Gaseous detector	-	150 µm	Barthe, N. et al, Nuclear Instruments and Methods in Physics Research, 2004.
Scintillating sheet	0.17 MBq/min	20 µm	Maskali, F. et al, Journal of nuclear cardiology, 2005.
Silicon sensor Medipix2	5.5 MBq/min	230 µm	Russo, P. et al. Physics in medicine and biology, 2008.

Characteristic of the method used for AR with ^{18}F.

Introduction

Difficulties of the autoradiography

- Range of positrons emitted from the tissue in the medium: water, silicon etc..

	Water	Silicon
250 keV	620 µm	333 µm
600 keV	2250 µm	1200 µm

- Limitation of the spatial resolution caused by scattering in the medium and longer β pathlengths due to kinetic energy
- Blurring effect

International Commission on Radiation Units and Measurements. Report 37. *Stopping Powers for Electrons and Positrons*

Introduction

Context

- Improve the visualisation using deconvolution algorithm
- Need to create a pseudo-PSF
- Ringing effect known as Gibbs phenomenon
- Bad quantitative intensity conservation

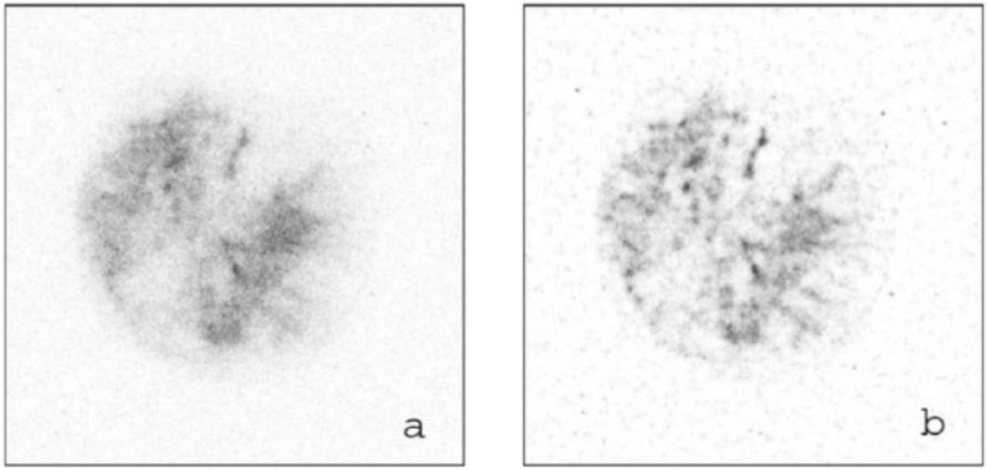

Deconvolution for tumor section image of HT29 human xenograft on nude rat containing hypoxia tracer ^{124}I-IAZGP (iodoazomycin galactopyranoside) . (a) Original DAR image of the tumor section. (b) Restored image using the R-L algorithm .

Zhang, Mutian, et al. *Medical physics*. 2008

Objective

- To perform autoradiography with CMOS sensor Mimosa-28, designed for high energy physics (the STAR PXL detector)
  - Spatial resolution 4 µm and efficiency 100% with MIP 120 GeV π- (Minimum Ionisation Particle)

- Improve the image with MLEM algorithm (Maximum Likelihood Expectation Maximization)
  - Conservation of the intensity after each iteration

Materials and methods

Fluorine 18

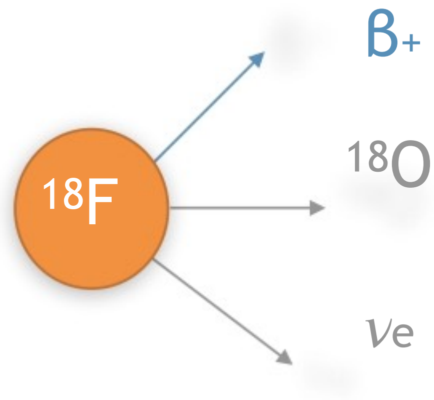

- A source of positrons β+ (97%)
- Half-life 109.8 min (≃ 2h)
- $E_{max\ \beta+}$ = 634 keV
- $E_{mean\ \beta+}$ = 250 keV

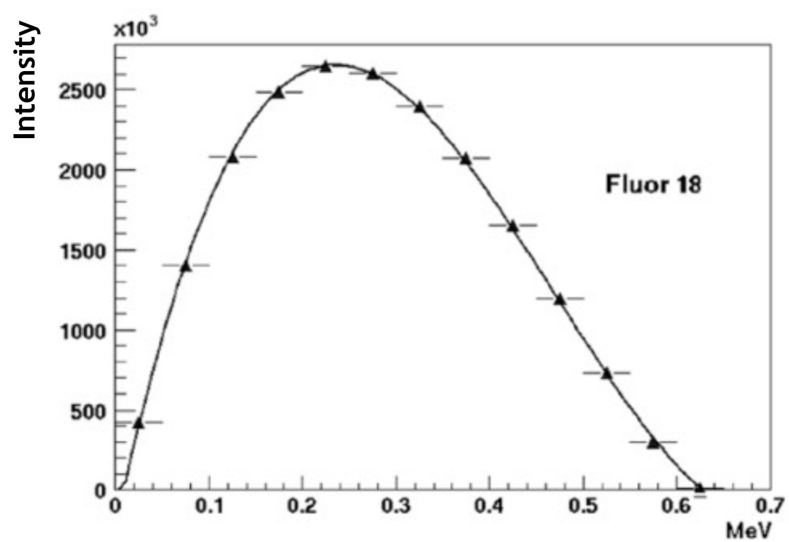

Jan, Sébastien, et al. *Ieee transactions on nuclear science*. 2005

Materials and methods

Radiotracer: 2-Deoxy-2-[18F]fluoroglucose (FDG)

- Radiotracer: coupling between radioactive atom and a vector
- FDG: analogue of glucose
- Metabolism of glucose in the cell tissue

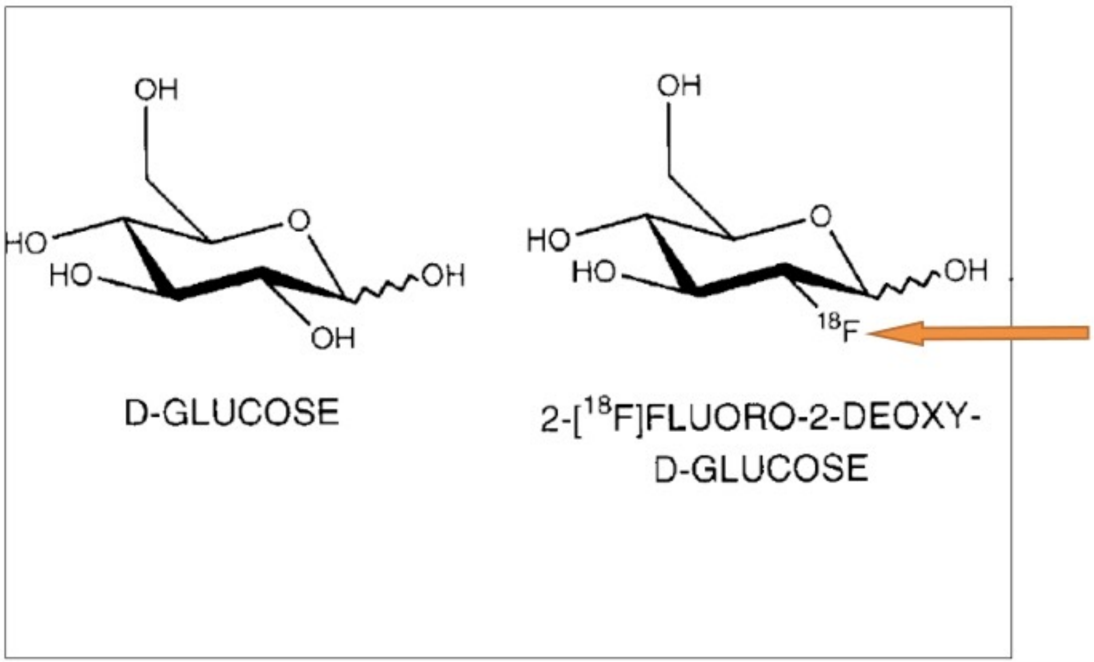

D. Le Bars. Revue de l'ACOMEN. 1998

Materials and methods

Mimosa-28, Minimum Ionizing particle MOS Active pixel sensor (IPHC)

Characteristics of the Mimosa-28

	Surface of detection	Pixel number	Pixel pitch	Epitaxial layer	511 keV ɣ interaction
Mimosa-28	3.8 cm^2	928 x 960	20.7 µm	15 µm	0.0283 %

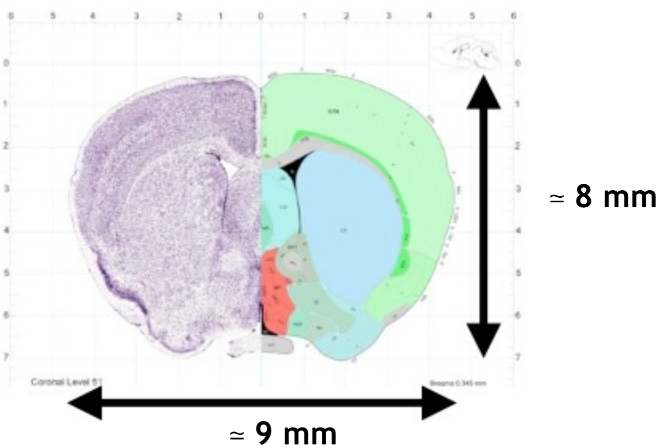

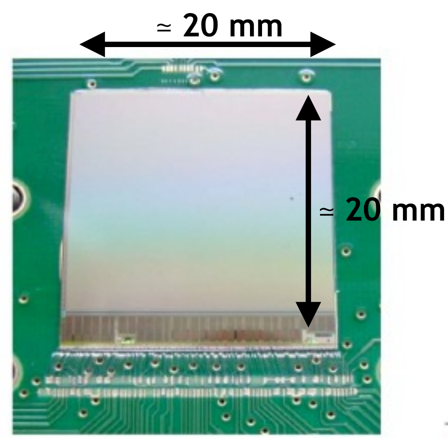

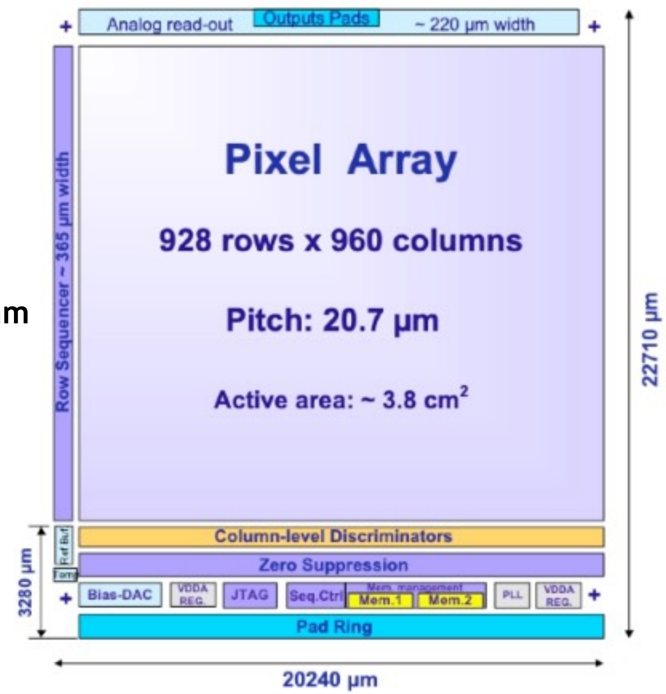

Valin, I. et al, Journal of Instrumentation, 2012

Materials and methods

Principle of detection

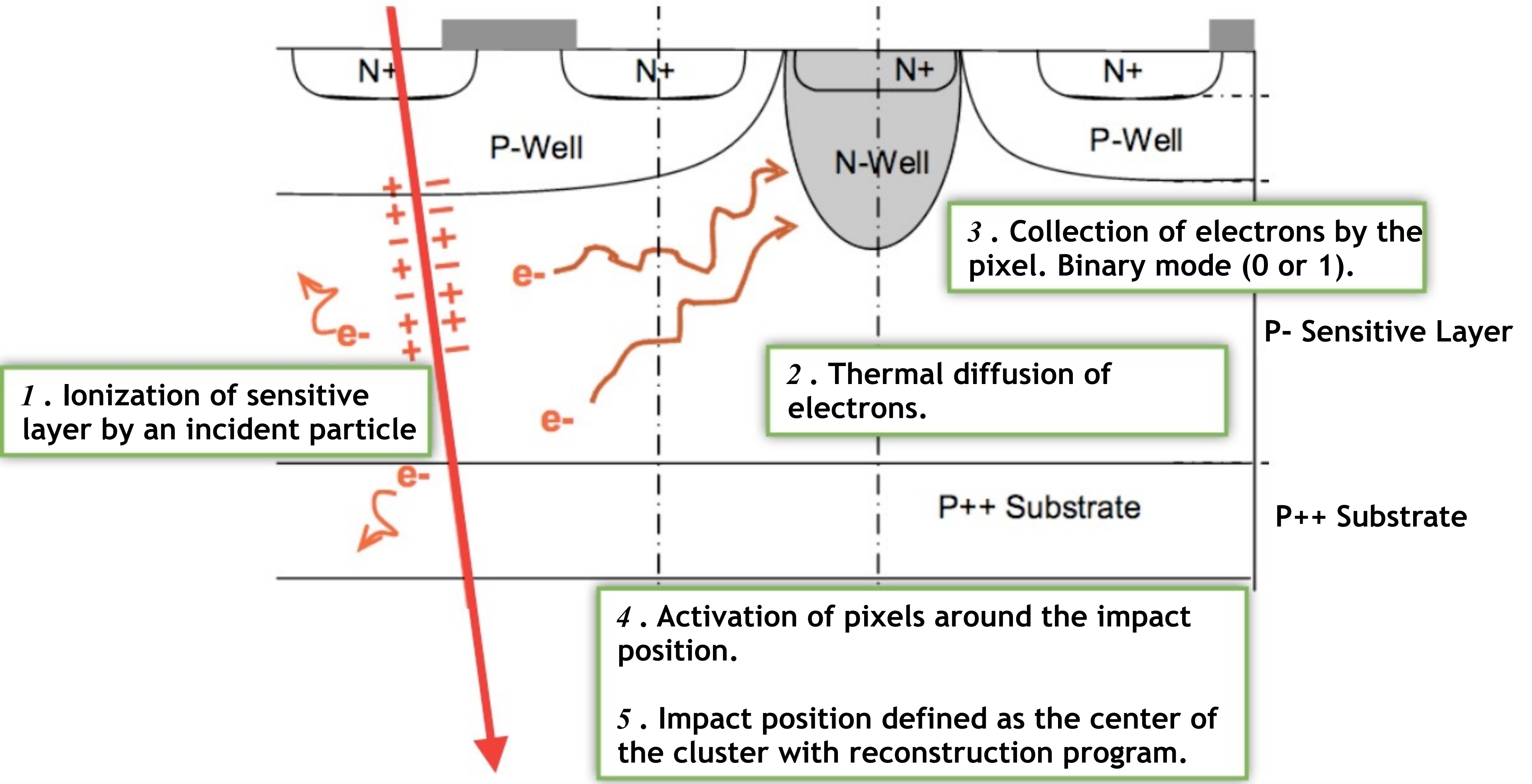

L. Yan, *Research and Development of Monolithic Active Pixel Sensors for the Detection of the Elementary Particles*, 2007

Materials and methods

Linearity and efficiency

- ^{18}F solution in a paper with a known activity measured by ISOMED2000
- Probability of β_+ emission 97%
- Counting the hits.sec_{-1} in function of the activity to test the linearity
- Efficiency: ratio between hit per sec / number β_+ per sec

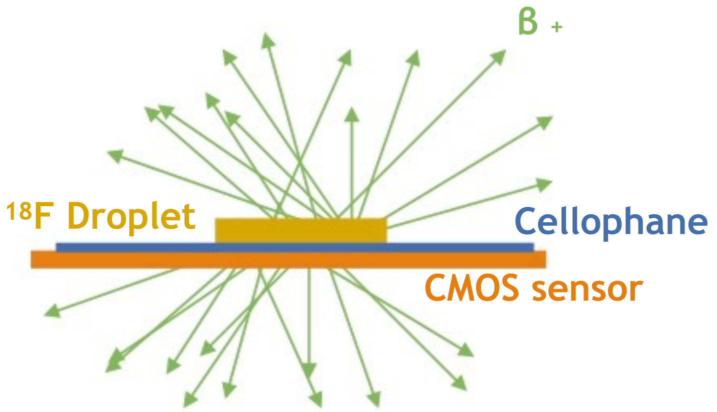

Materials and methods

Spatial resolution, capacity of a system to distinct two closest points sources

- Experimental setup:

absorbing edge method

- Variable distance between source and sensor.
- Source ^{18}F between two microscope slides.

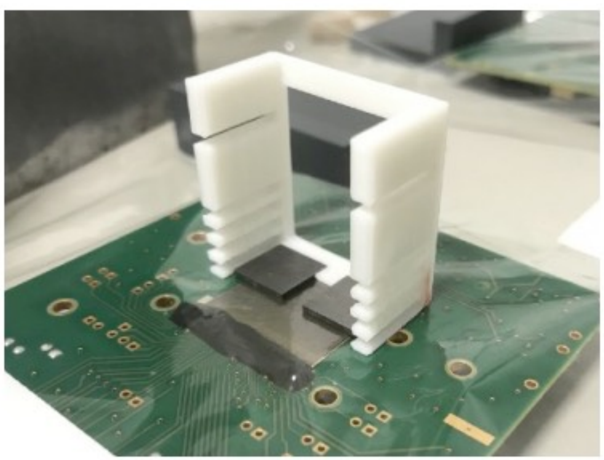

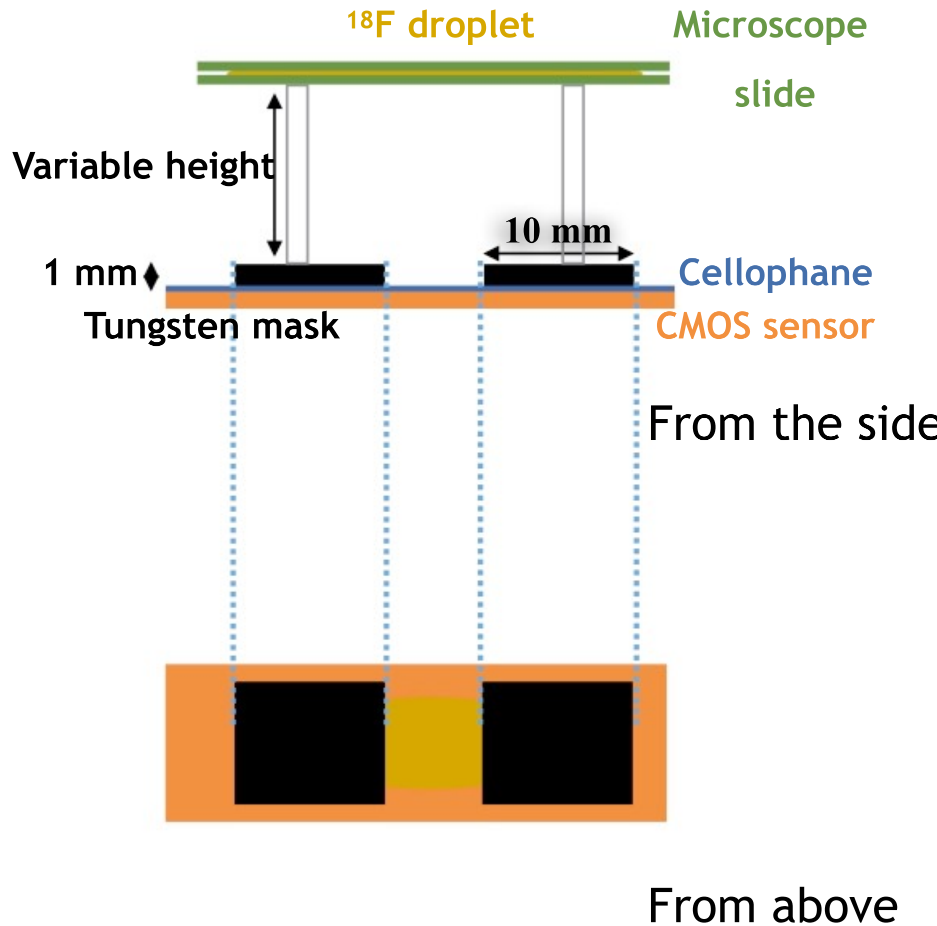

Lauria, Adele, et al. Nuclear Instruments and Methods in Physics Research Section A: Accelerators, Spectrometers, Detectors and Associated Equipment. 2007

Materials and methods

Spatial resolution, capacity of a system to distinct two closest points sources

- ERF (Edge Response Function) with the projection on x-axis.

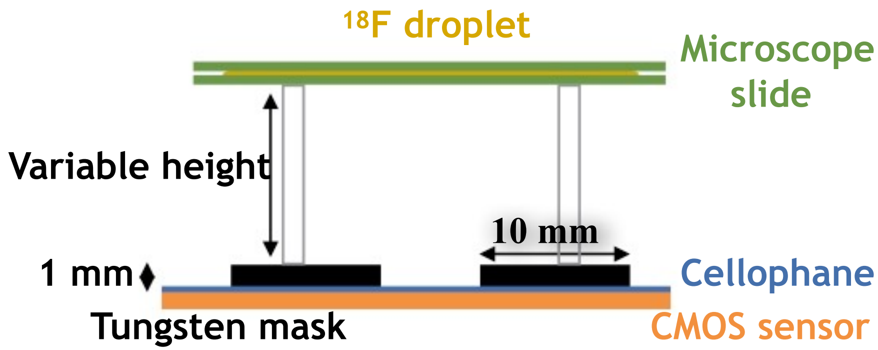

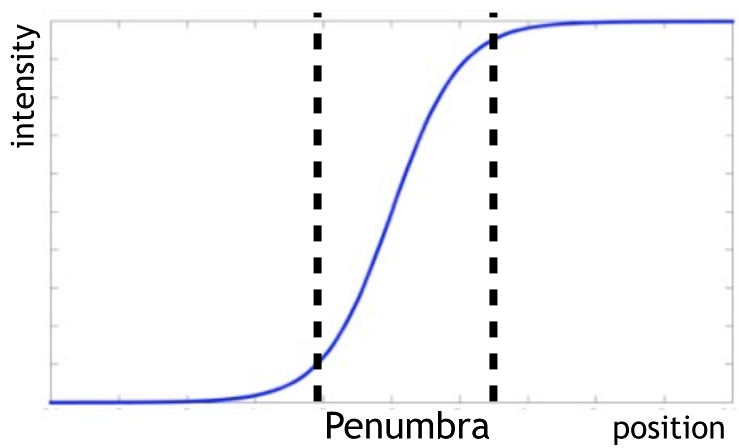

$$ERF(x) = \frac{1}{2}\left(1+\mathrm{erf}\left(\frac{x-\mu}{\sigma\sqrt{2}}\right)\right)$$

$$FWHM = 2.3548\sigma$$

Materials and methods

Autoradiography with PET scan

- Injection of FDG by intravenous in mouse:
  - age: 11 weeks
  - weight: 38,7 ± 0.1 g
  - fasted: 5 h
  - activity: 35 MBq ± 5 % /200 µL

1 h biodistribution →

- PET scan:
  - IRIS Inviscan (spatial resolution 1 mm at the center)
  - Acquisition time 10 min

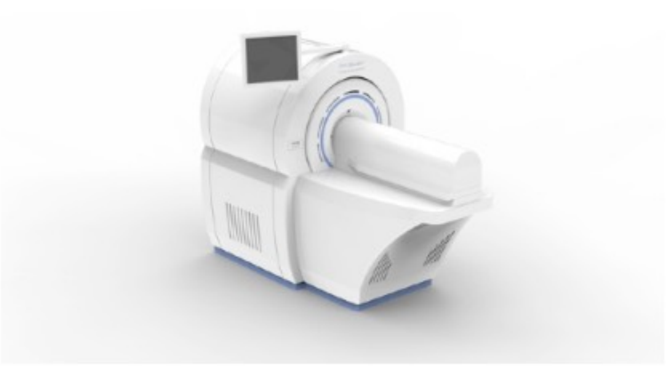

Brain removal ↙

- Weight: 402,8 ± 0.1 mg
- Activity: 407 kBq ± 5 %
- Cut the brain into section 50 µm with vibratome Leica VT1200 S
- Optical image of the block face with a camera Canon macro lens
- Putting the slice on the Mimosa-28 sensor

***according to the animal ethics committees CREMEAS, Strasbourg, France**

Materials and methods

Reconstruction algorithm

- Object F, distribution of the radiotracer in the tissue.
- Transformation R , modelled by the interaction of the positrons with the sensor and the medium.
- Image p_j .

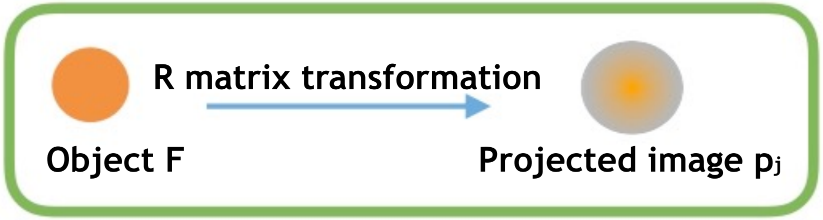

Lange, Kenneth, and Richard Carson. *J. Comput. Assist. Tomogr.* 1984

Materials and methods

Reconstruction algorithm

- Iterative reconstruction MLEM (Maximum Likelihood Expectation Maximisation) introduced by K. Lange and R. Carson
- *F* estimated object
- *R* matrix of the system
- *P* projected image

$$\hat{F}_i^{(n+1)} = \frac{\hat{F}_i^{(n)}}{\sum_j R_{ji}} \sum_j R_{ji} \frac{p_j}{\sum_k R_{jk} \hat{F}_k^{(n)}}$$

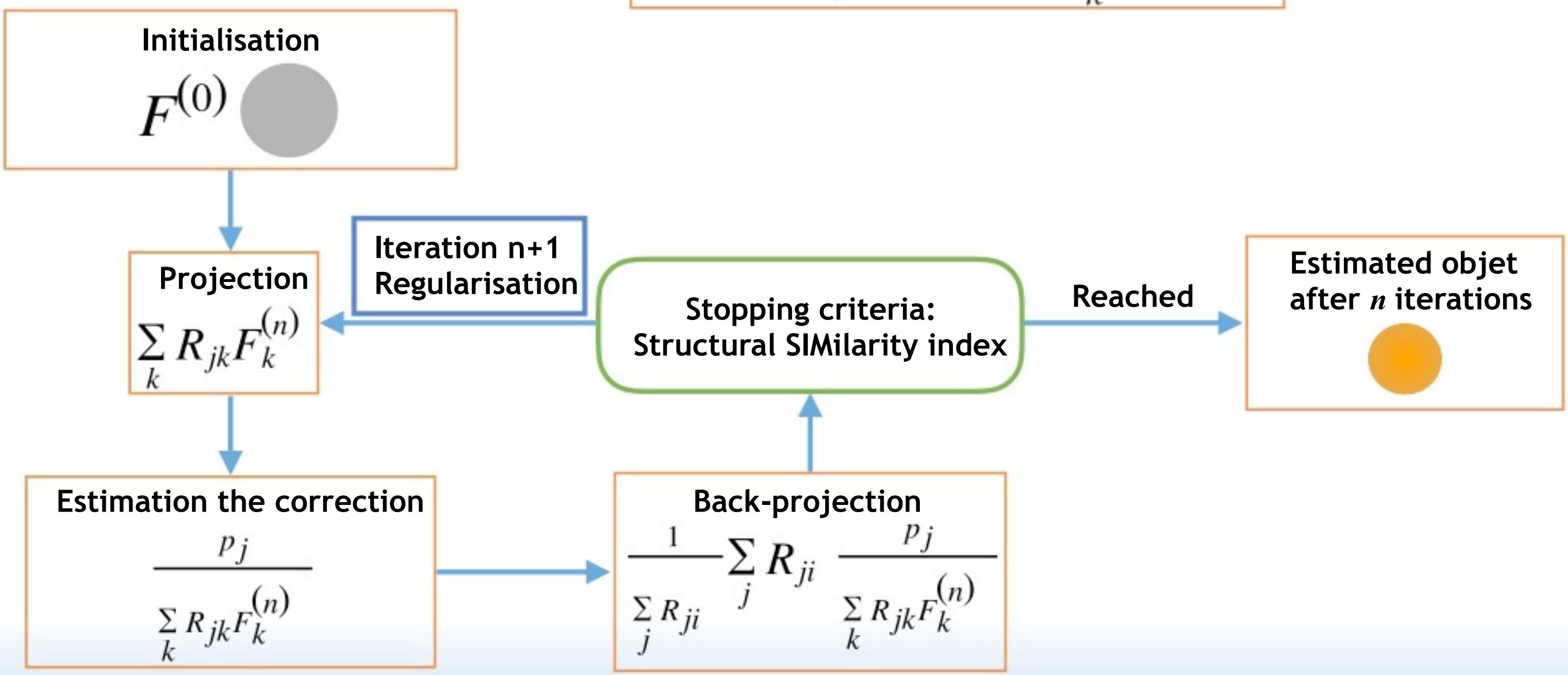

Lange, Kenneth, and Richard Carson. *J. Comput. Assist. Tomogr.* 1984

Materials and methods

Creation matrix of the system

- *R* matrix of the system: probability to detect in the pixel *j* (sensor) a positron emitted from a voxel *i* (tissue) with an isotropic and uniform emission

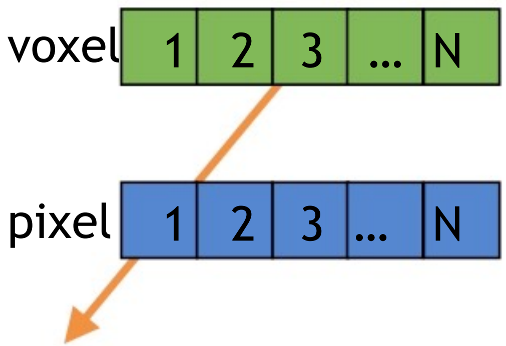

A positron emitted from the voxel 3 and detected in the pixel 1.

$$R_{ji} = \frac{N_j^D}{N_i^E}$$

with

N_j^D	Number of positrons detected in the pixel j .
N_i^E	Number of positrons emitted from the voxel i .

Materials and methods

Creation matrix of the system

- Simulation Monte-Carlo GATE to generate the positrons and the interaction with the sensor using Penelope model
- 1 billion positrons emitted with kinetic energy following ^{18}F energy spectrum

- Modelling the response of the sensor (electron's diffusion in the sensitive layer, Janesick's model)

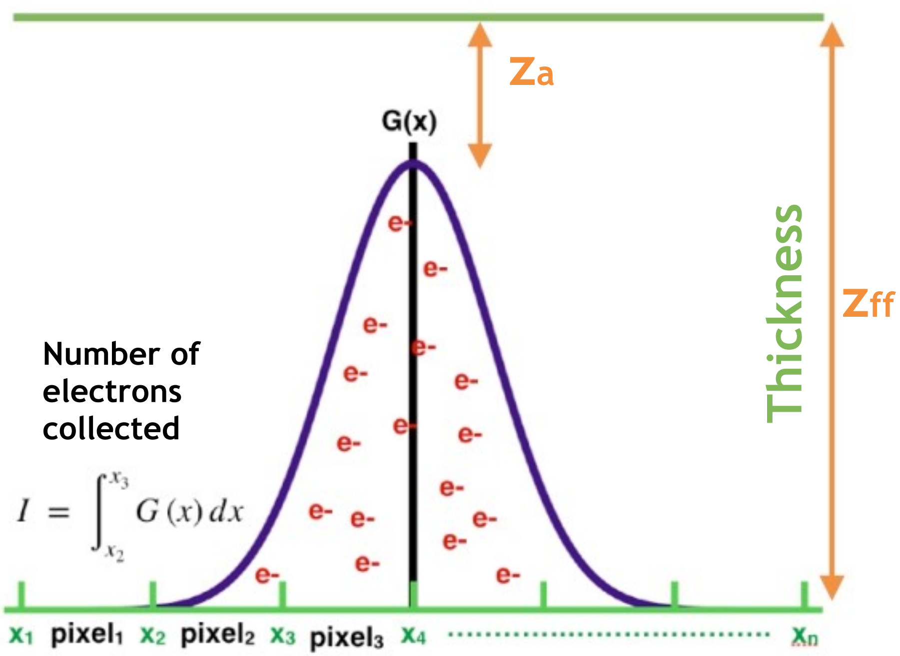

$$\sigma_{tot} = \sqrt{\sigma_{ff}^2 + \sigma_i^2}$$

$$\sigma_{ff} = \frac{z_{ff}}{2}\sqrt{1 - \left(\frac{z_a}{z_{ff}}\right)^2}$$

$$\sigma_i = 0{,}0062E^{1{,}75}$$

Baro, J., et al. Nuclear Instruments and Methods in Physics Research, 1995
Cabello, Jorge, and Kevin Wells, Physics in Medicine & Biology, 2010

Results and discussion

Linearity, efficiency and spatial resolution

- 44.2 ± 0,4 % (0.44 counts/sec/Bq) with an activity between 3 kBq and 400 kBq
- Solid angle lower than 2π sr
- Loss signal caused by dead layers: paper, electronic parts

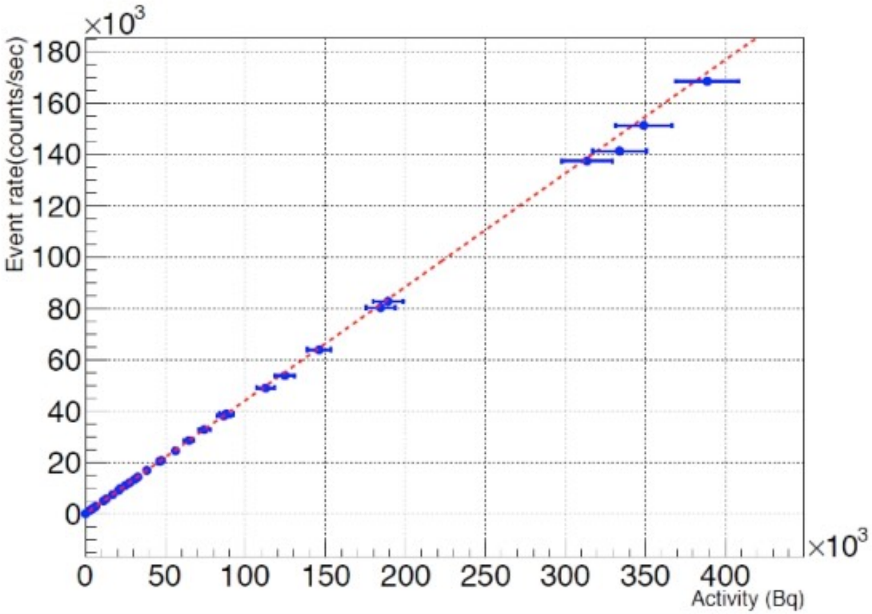

Results and discussion

Linearity, efficiency and spatial resolution

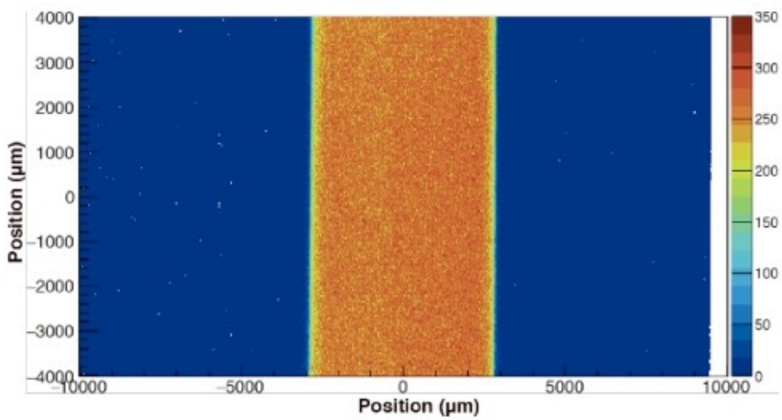

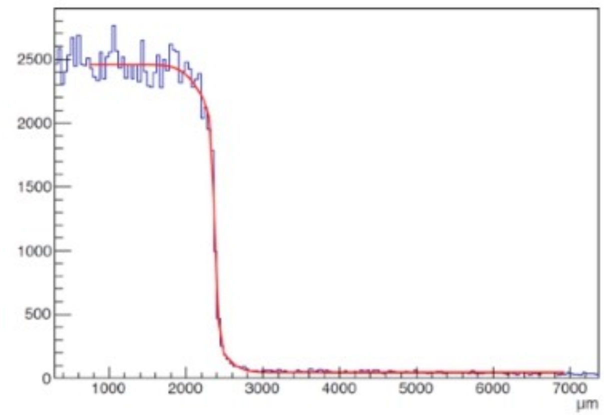

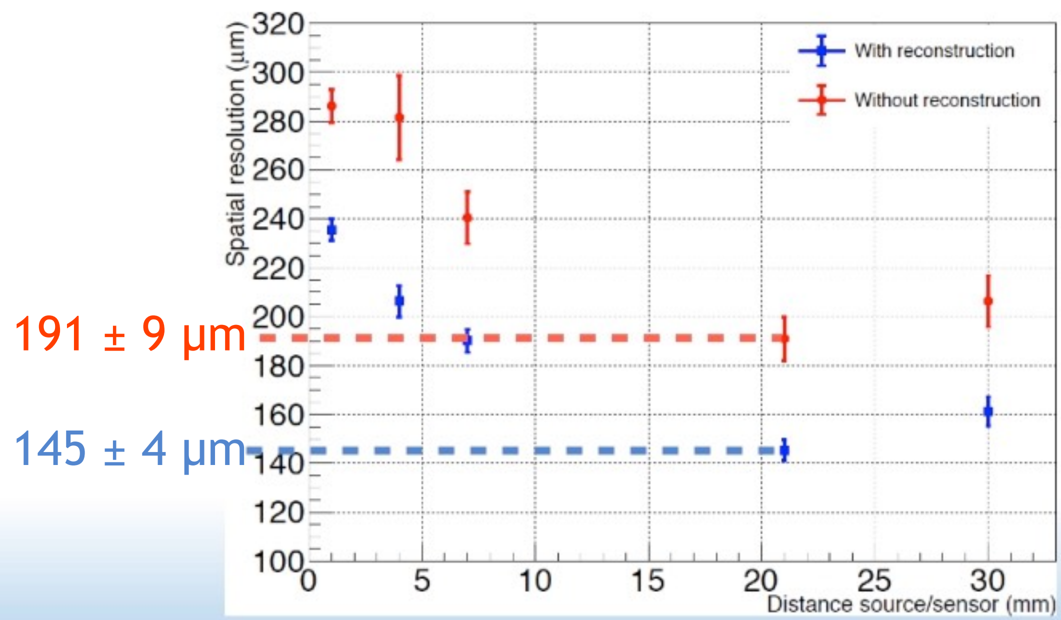

- Better spatial resolution at 20 mm and 30 mm
- Interaction of positrons with high kinetic energy and a normal angle to the surface
- Tungsten mask: role of collimator
- Secondary emission from the mask: electrons and photons

Results and discussion

Autoradiography with PET scan

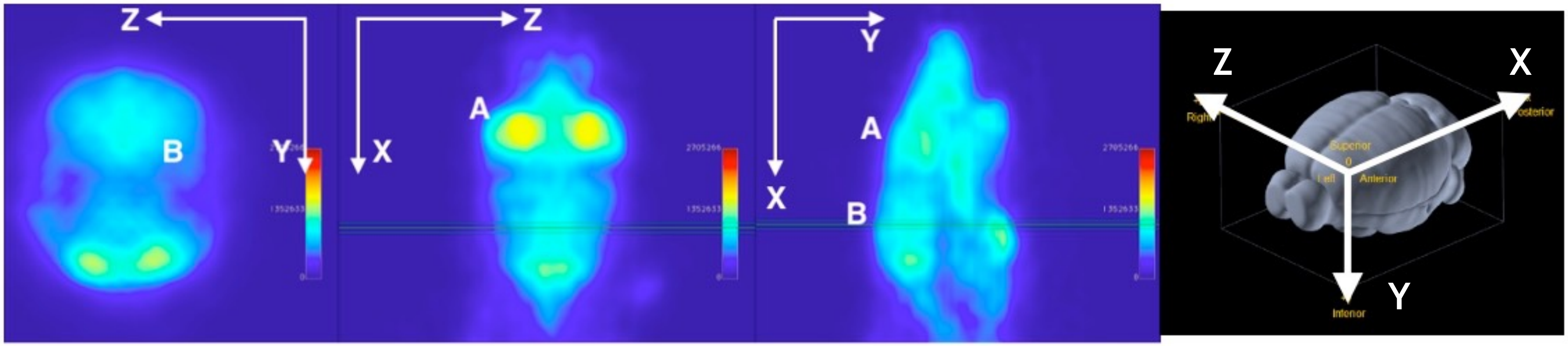

Transverse Coronal Sagittal

Biodistribution of 18F-FDG after 1 h biodistribution with 10 min acquisition time. A : Eye, B : Brain

- Important uptake in the eyes. Consumption of glucose by the Harderian gland in the eye stimulated by the light
- Homogenous uptake in the brain with the PET scan caused by the limitation of the spatial resolution

Results and discussion

Autoradiography with PET scan

- Specific uptake in different region of the brain section (striata, cortex)

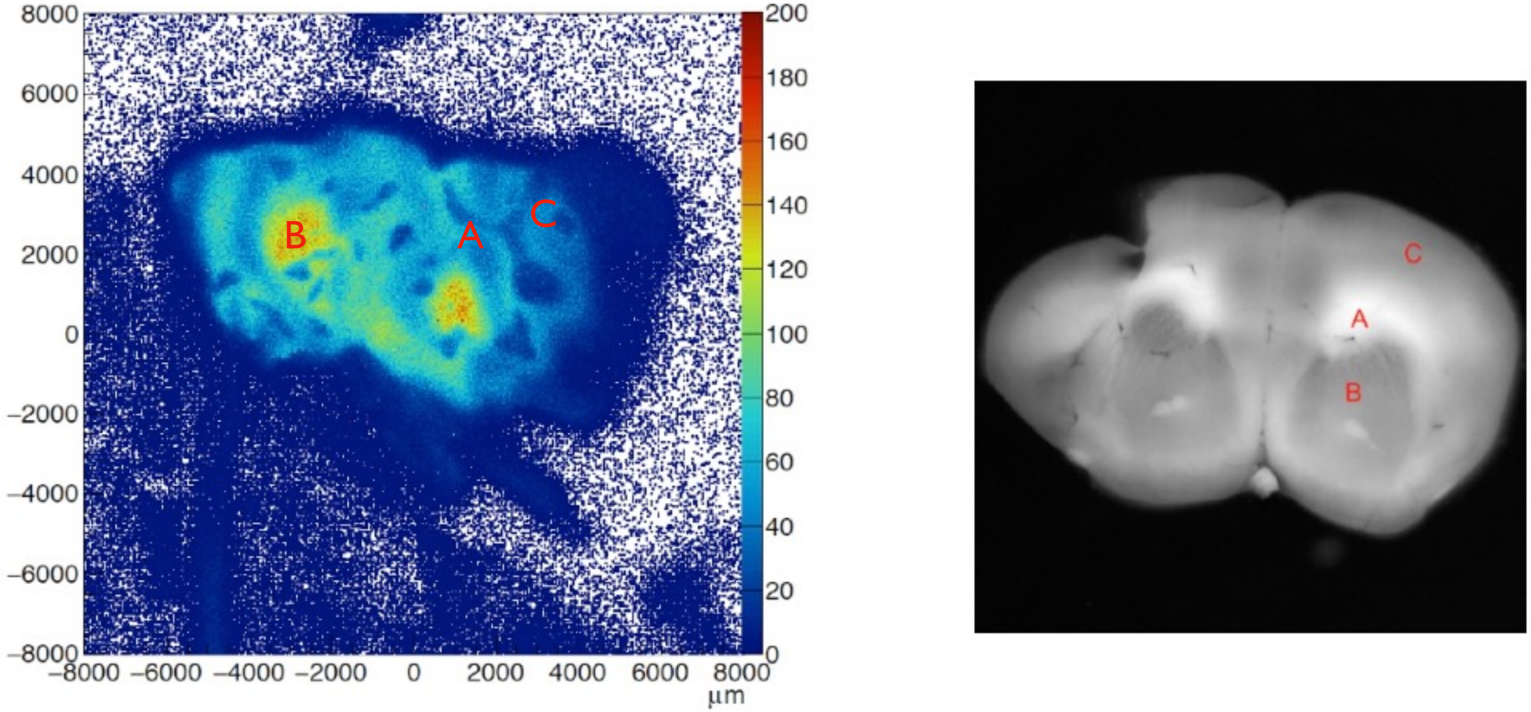

(a) Autoradiography of the brain section 50 μm with 2 h acquisition time. Colour bar represents the number of hits in the pixel. (b) Optical image of the cross-section. A : corpus callosum, B : striata, C : cortex.

Results and discussion

Autoradiography with PET scan

- Specific uptake in different region of the brain section (striata, cortex)

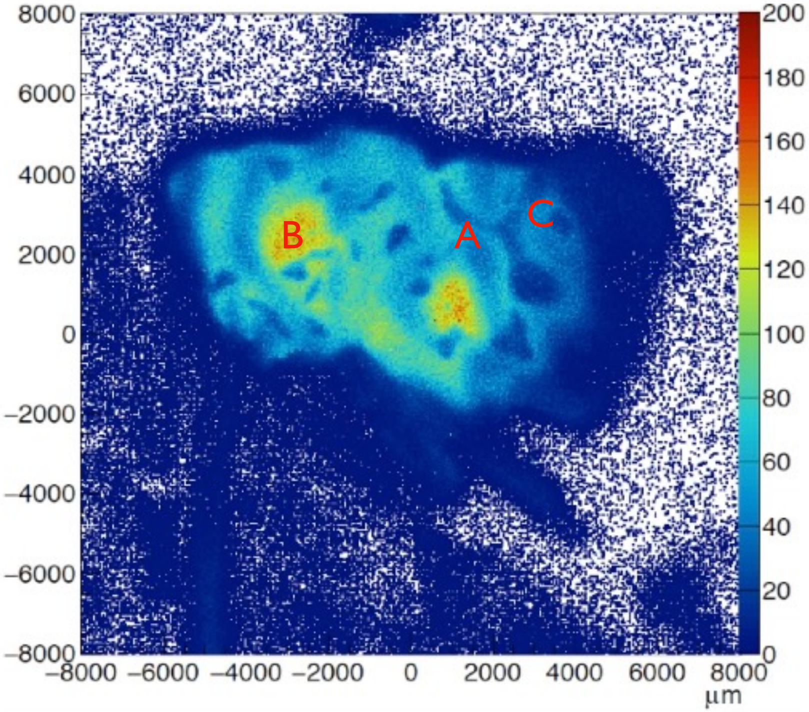

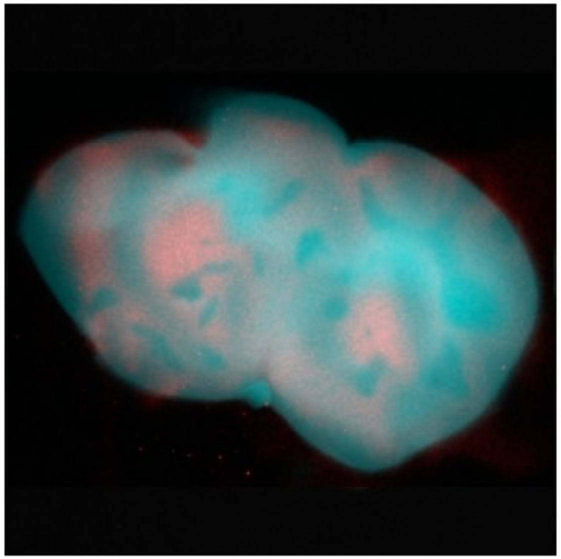

(a) Autoradiography of the brain section 50 µm with 2 h acquisition time. Colour bar represents the number of hits in the pixel. (b) Optical image of the cross-section. A : corpus callosum, B : striata, C : cortex.

Results and discussion

MLEM algorithm

- Stopping criteria: SSIM (Structural Similarity Index)
- Stabilisation of the SSIM after 100 iterations

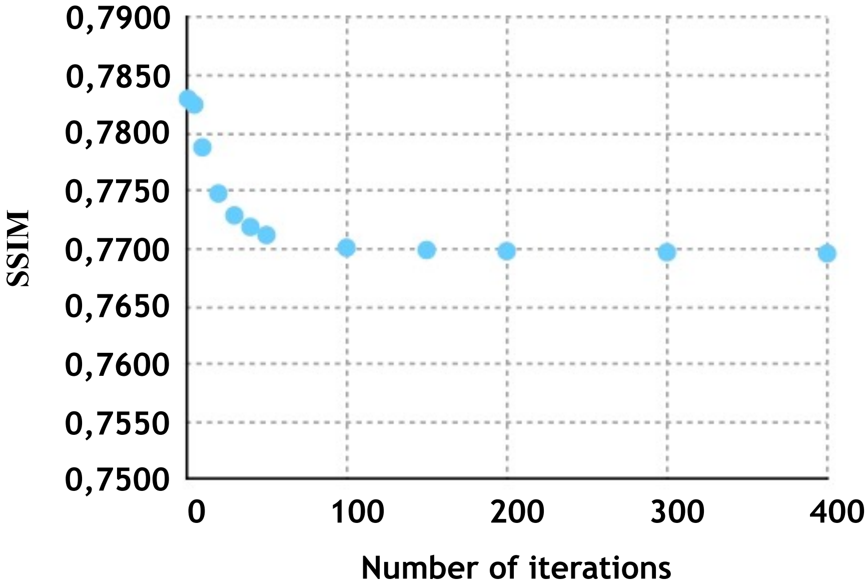

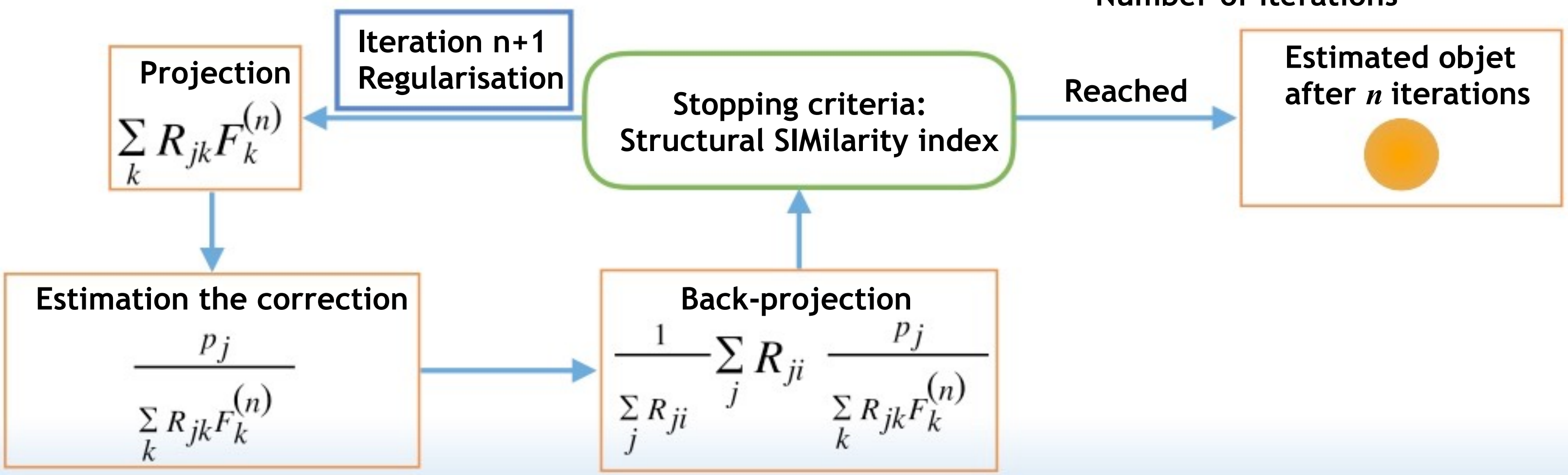

Results and discussion

Autoradiography with PET scan

- Specific uptake in different region of the brain section
- Improve the sharpness with MLEM algorithm (limit of the tissue, morphologie)
- Reduction of the scattering (blurring effect)
- Regularisation to decrease noise

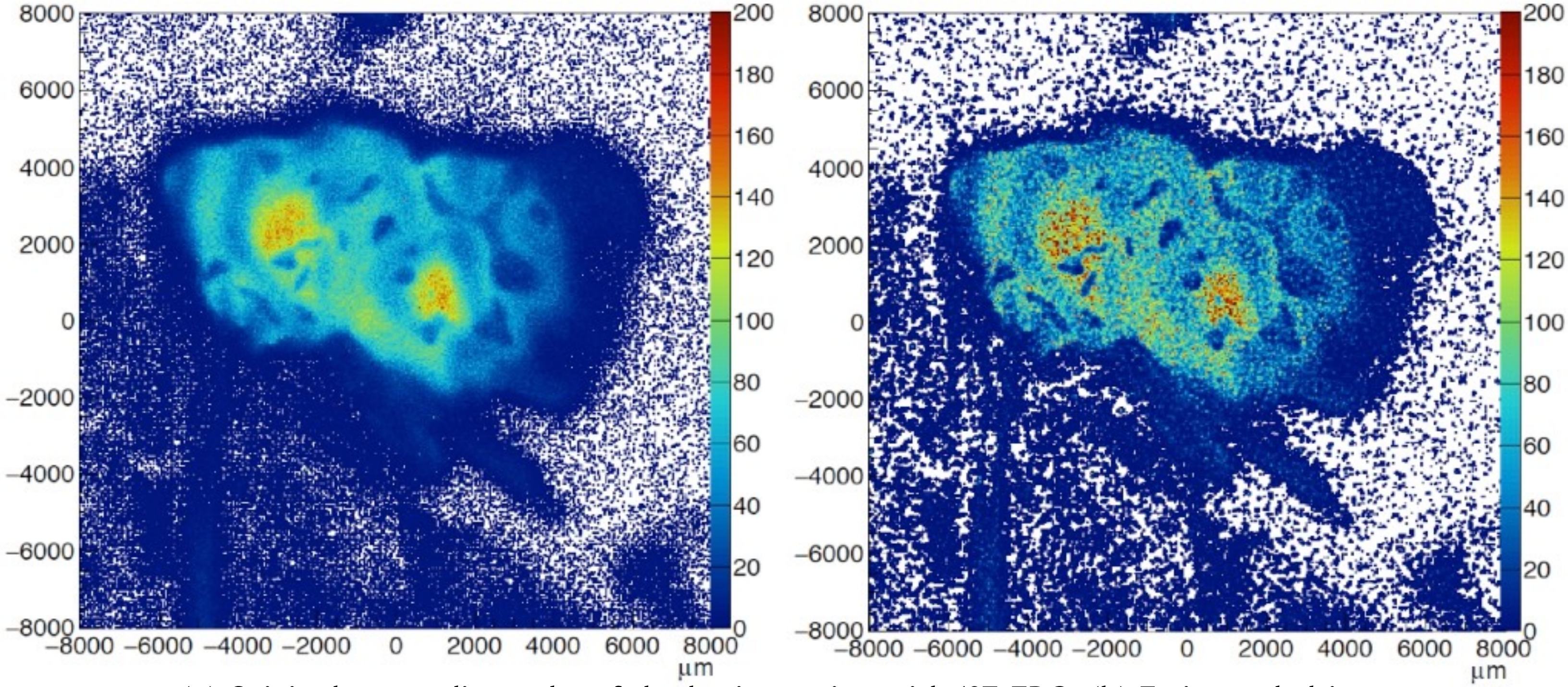

(a) Original autoradiography of the brain section with ^{18}F-FDG. (b) Estimated object using the MLEM algorithm with 100 iterations, regularisation FWHM = 30 µm.

Conclusions and perspective

- Autoradiography: a method to visualise at brain scale
- Good efficiency and a spatial resolution similar with the others systems
- Multimodality: PET scan and autoradiography (functional imaging) with the same radiotracer, and optical imaging (anatomical imaging)
- MLEM algorithm: increasing the sharpness in the image by decreasing the blurring effect cause by the scattering of the particles

- Measure the performance of the MLEM algorithm (uniformity, efficiency, spatial resolution)

Thank you for your attention

We thank the PICSEL group for providing the technical support. We thank Lionel Thomas, Bruno Jessel for the help with the mouse and the MI-CNRS Imag'In for financial support.

truong.nguyen-pham@iphc.cnrs.fr

Acknowledge

We thank the PICSEL group for providing the technical support. We thank Lionel Thomas, Bruno Jessel for the help with the mouse and the MI-CNRS Imag'In for financial support.

Multiple scattering

$$\theta_0 = \frac{13.6\ \mathrm{MeV}}{\beta c p}\, z \sqrt{x/X_0}\Big[1 + 0.038 \ln(x/X_0)\Big]$$

Source : PDG

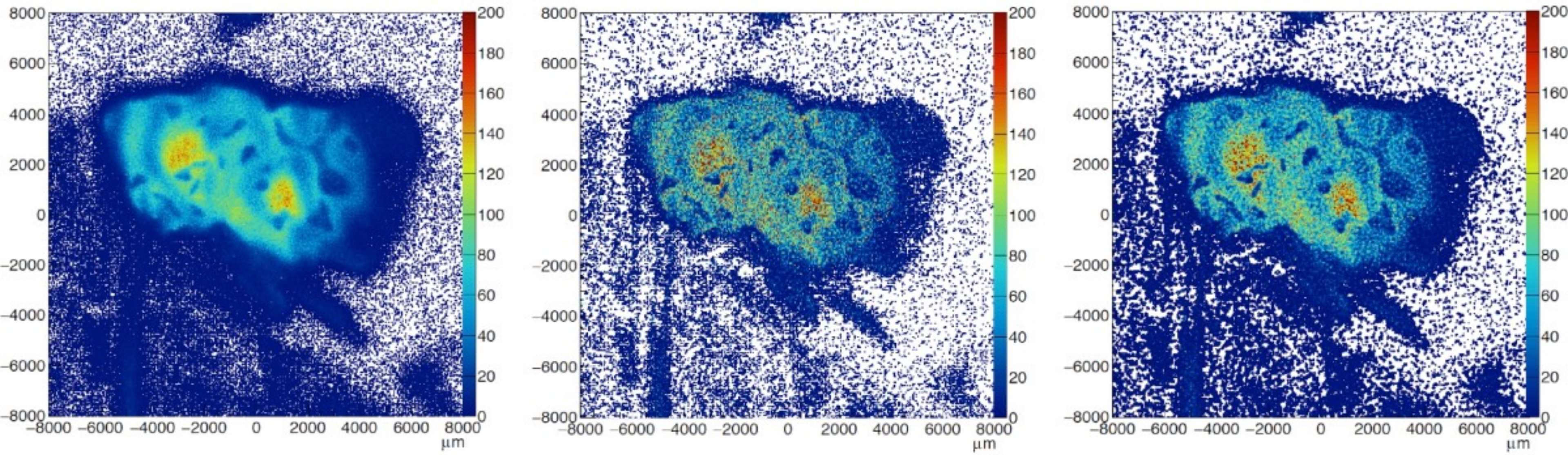
8000
6000
4000
2000
0
−2000
−4000
−6000
−8000
−8000 −6000 −4000 −2000 0 2000 4000 6000 8000
μm
200
180
160
140
120
100
80
60
40
20
0

AR Fusion

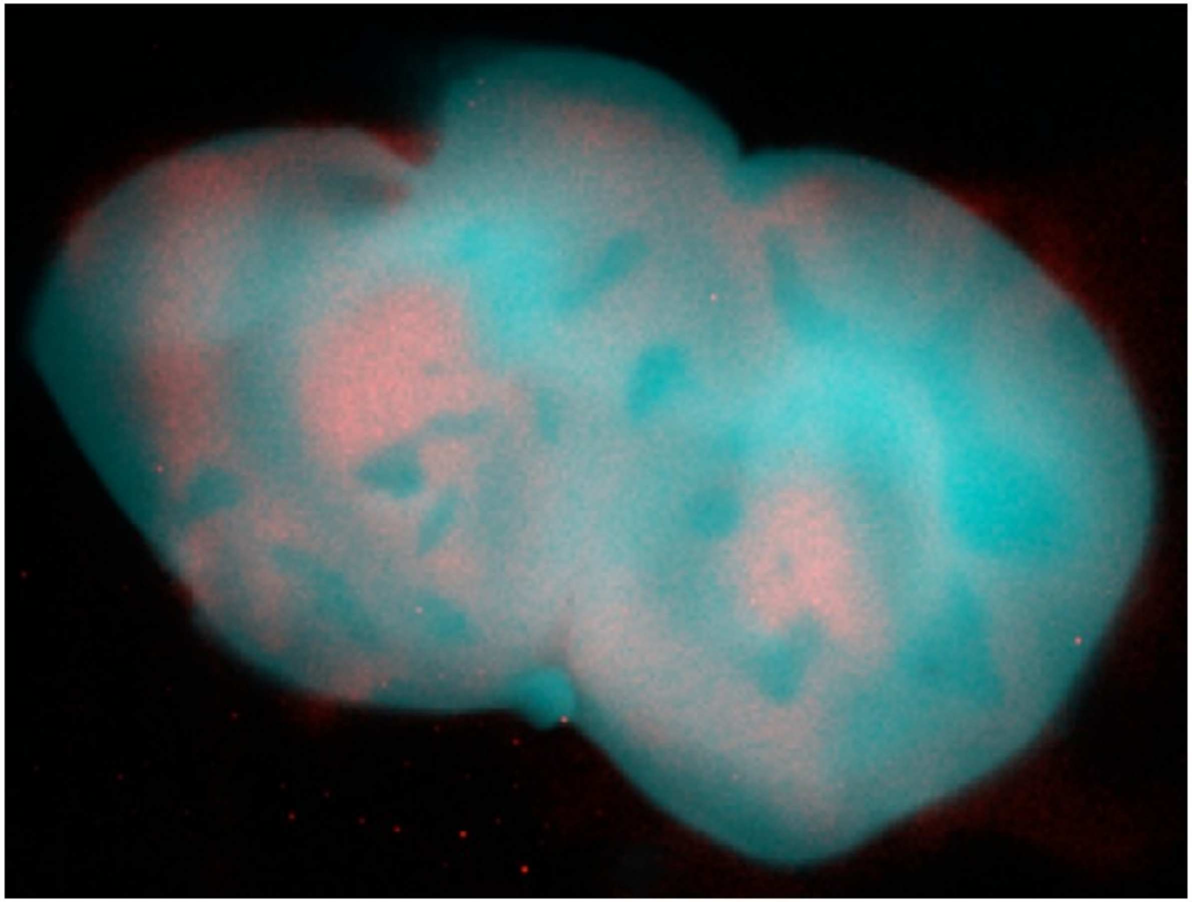

Results and discussion

Linearity, efficiency and spatial resolution

- Efficiency : attenuation in the medium: paper, film, dead layer.
- Resolution : diffusion of β + in the medium, secondary emission (photons and low electrons).

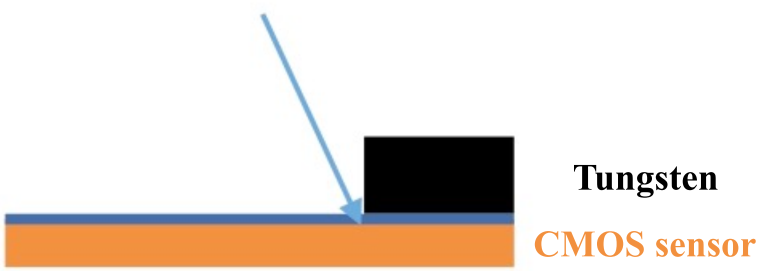

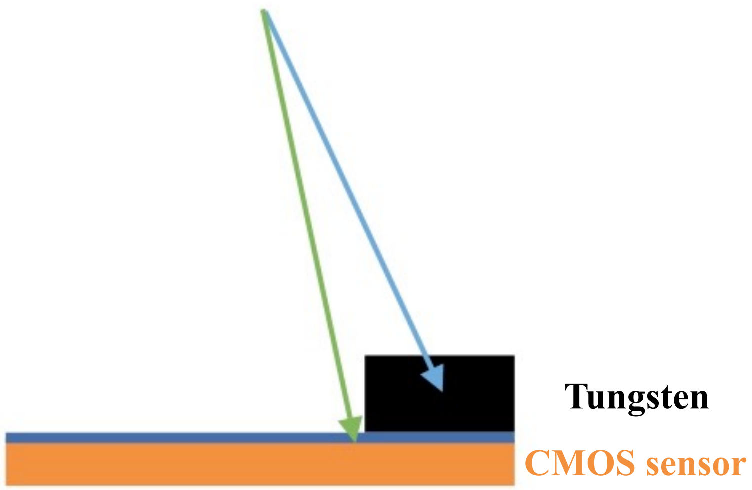

Spatial resolution vs dimension sensor

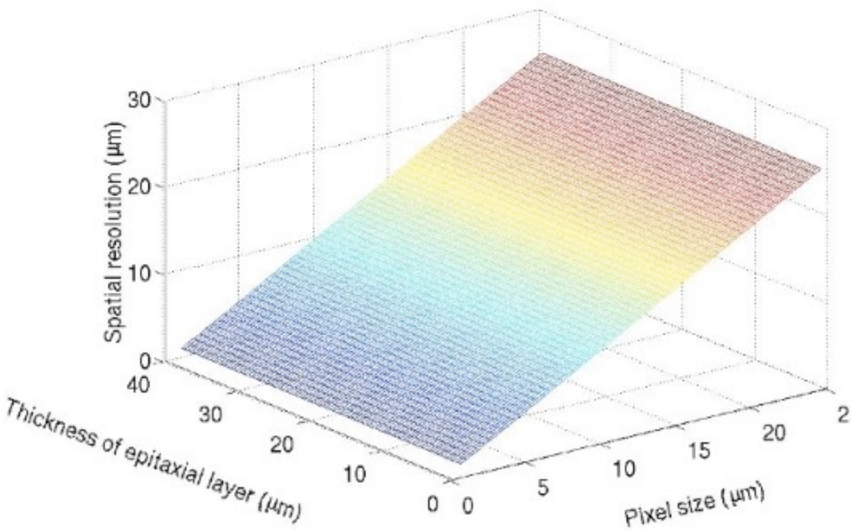

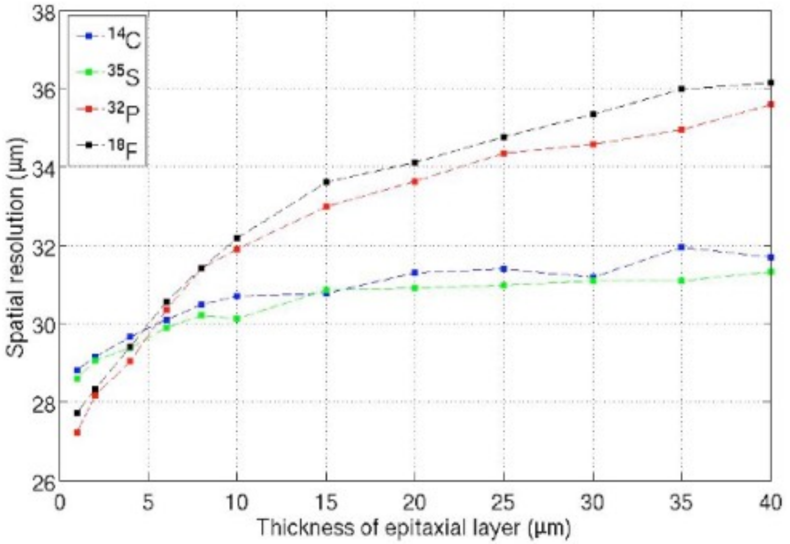

Cabello, J., & Wells, K., *A Monte Carlo investigation into the fundamental limitations of digital β -autoradiography: Considerations for detector design* , 2007.

Emulsion film

- Deposition of energy in the film.
- Metallization of silver halide crystals.
- Revelation step

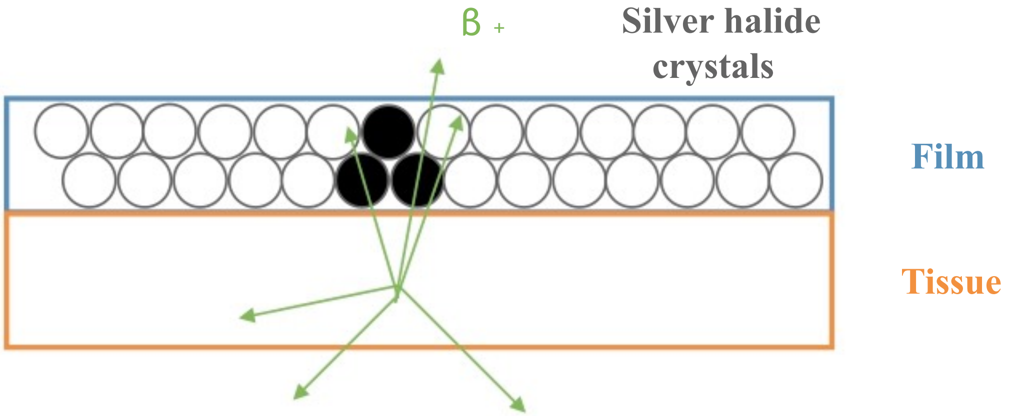

Emulsion film

- Deposition of energy in the film.
- Metallization of silver halide crystals.
- Revelation step

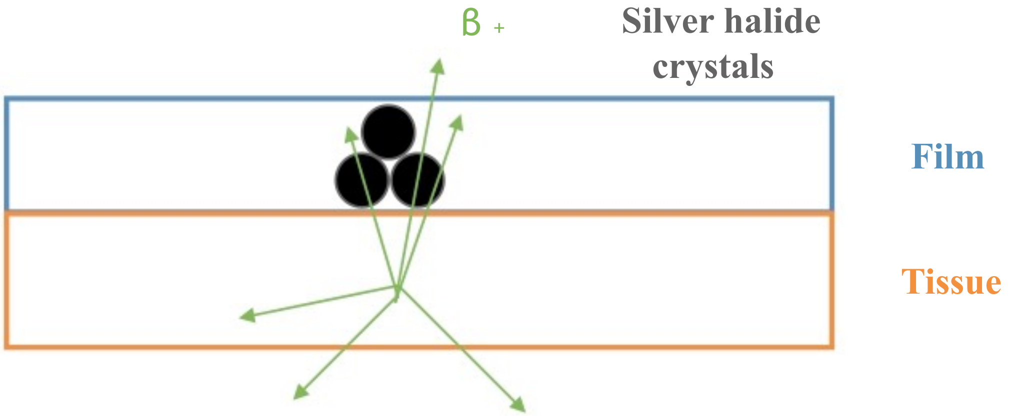

Phosphor plate

- Electron excited by an incidence particle.
- Trapped in a trap state.
- Liberation by a laser beam.
- Deexcitation of electron.
- Emission a visible photon.

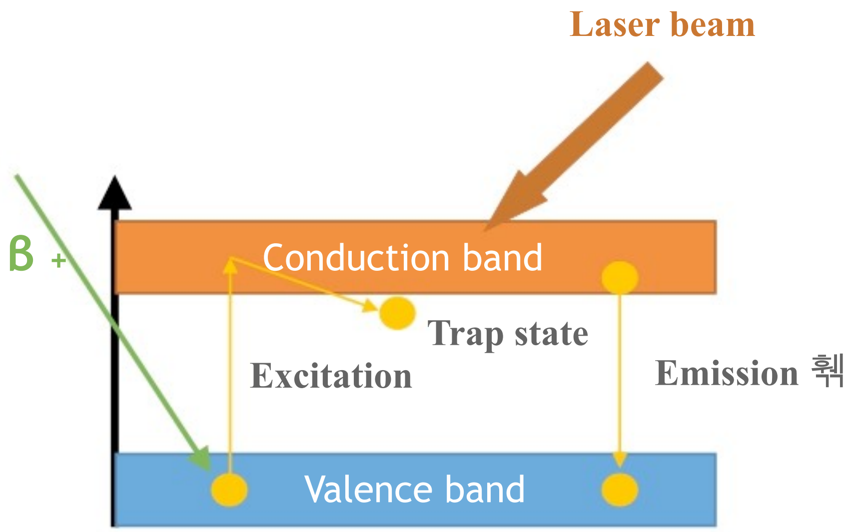

Gaseous detector

- Ionisation of the gas by an incidence particle.
- Acceleration and multiplication of the electrons by an electric field.

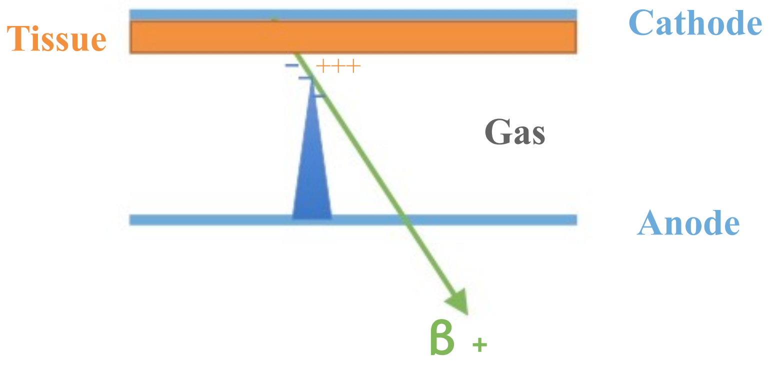

Scintillating sheet

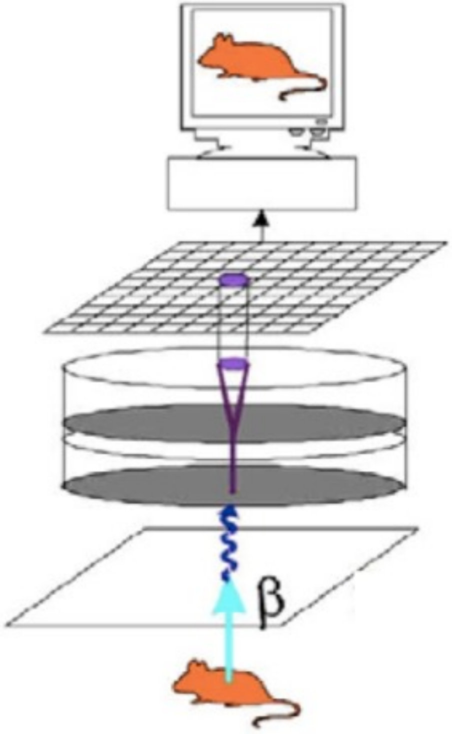

GATE Simulation

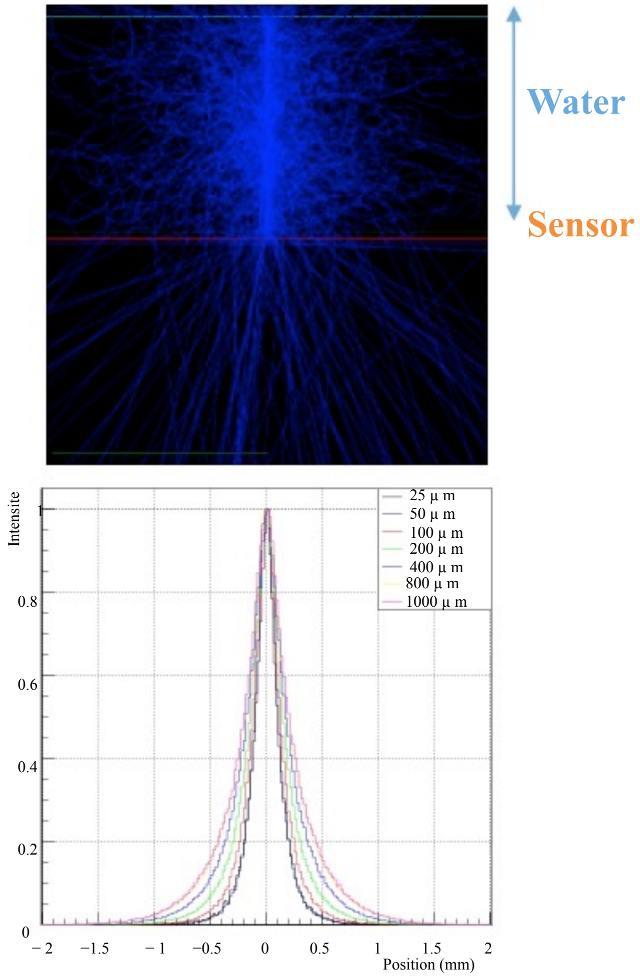

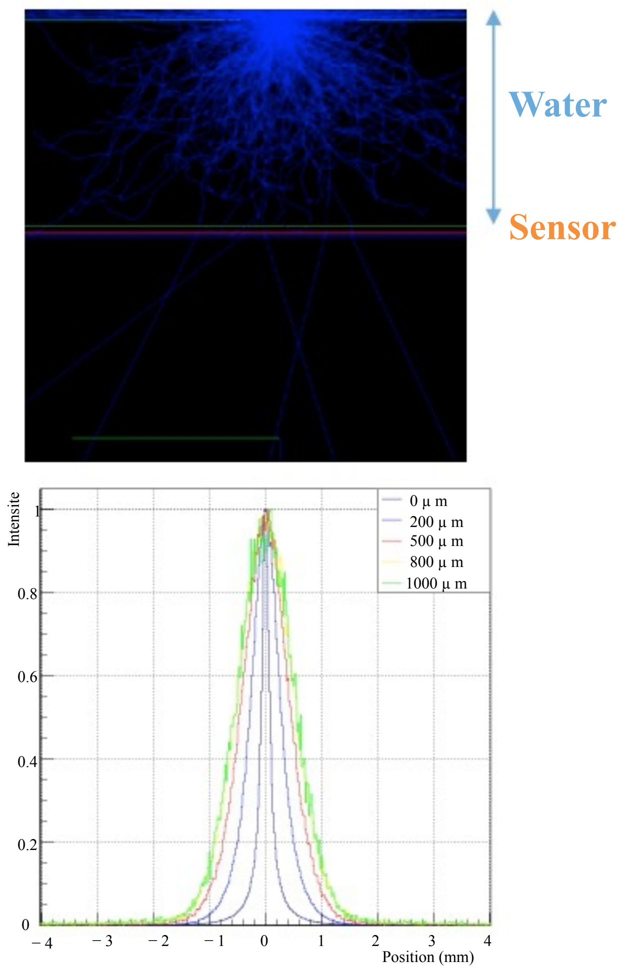

State of art autoradiography

Technique AR	Activity injected per acquisition time	Spatial resolution	Author
Emulsion film	0.77 MBq/min	4 µm	Yamada, S. et al, Neuroscience letters, 1990.
Phosphor imaging plate	1 MBq/min	330 µm	Mizuma, H. et al, Journal of Nuclear Medicine, 2010.
Gaseous detector	-	150 µm	Barthe, N. et al, Nuclear Instruments and Methods in Physics Research, 2004.
Scintillating sheet	0.17 MBq/min	20 µm	Maskali, F. et al, Journal of nuclear cardiology, 2005.
Silicon sensor Medipix2	5.5 MBq/min	230 µm	Russo, P. et al. Physics in medicine and biology, 2008.

Characteristic of the method used for AR with ^{18}F.

State of art autoradiography

Technique AR	Activity injected per acquisition time	Spatial resolution	Author
Emulsion film	0.77 MBq/min	4 µm	Yamada, S. et al, Neuroscience letters, 1990.
Phosphor imaging plate	1 MBq/min	330 µm	Mizuma, H. et al, Journal of Nuclear Medicine, 2010.
Gaseous detector	-	150 µm	Barthe, N. et al, Nuclear Instruments and Methods in Physics Research, 2004.
Scintillating sheet	0.17 MBq/min	20 µm	Maskali, F. et al, Journal of nuclear cardiology, 2005.
Silicon sensor Medipix2	5.5 MBq/min	230 µm	Russo, P. et al. Physics in medicine and biology, 2008.

Characteristic of the method used for AR with ^{18}F.

Introduction

Difficulties of the autoradiography

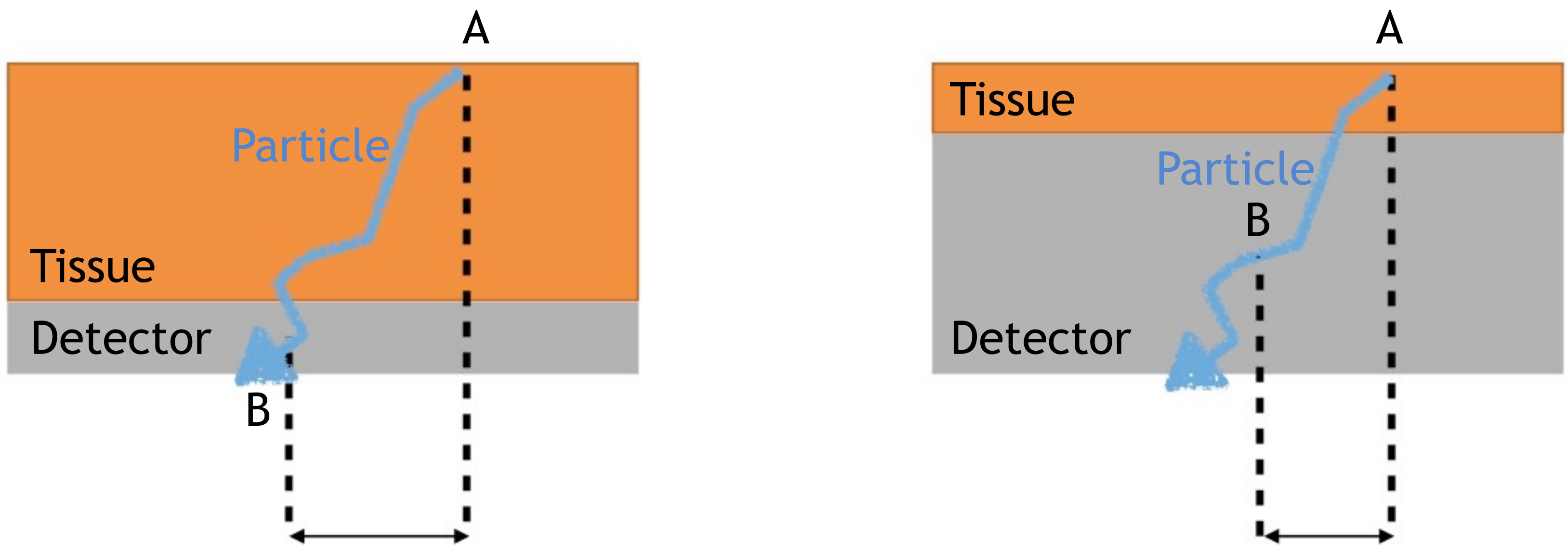

Multiple scattering modifies the trajectory of a charged particle.

Introduction

Difficulties of the autoradiography

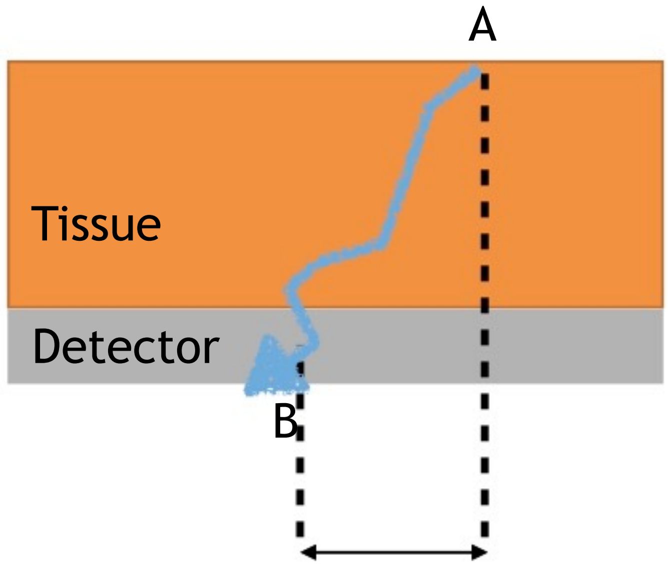

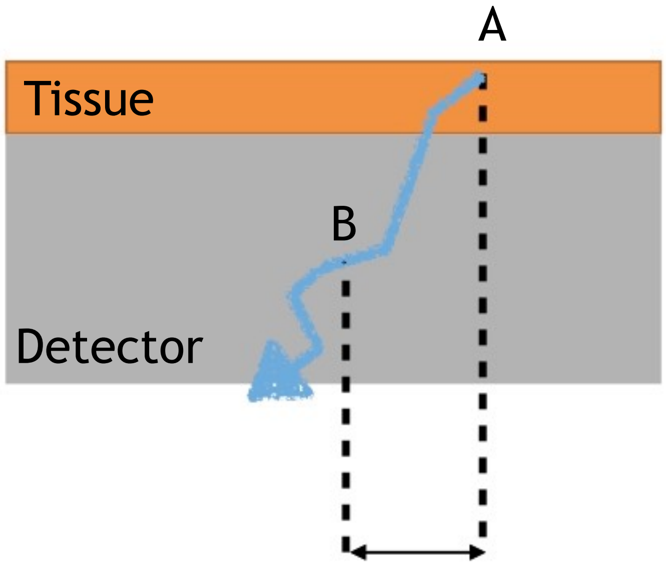

Thickness reduction of the tissue and the sensor